

# THE UNIVERSITY OF MICHIGAN

## COLLEGE OF ENGINEERING DEPARTMENT OF AEROSPACE ENGINEERING

### Progress Report

## Fluid Mechanics of Magnetically Balanced Arcs in Cross Flows

GPO PRICE \$ \_\_\_\_\_

CFSTI PRICE(S) \$ \_\_\_\_\_

A.M. KUETHE

Hard copy (HC) 3.00Microfiche (MF) .65

ff 653 July 65

### Supported by:

National Aeronautics and Space Administration  
Grant No. NGR-23-005-128  
Washington, D. C.

Administered through:

September 1967

## OFFICE OF RESEARCH ADMINISTRATION • ANN ARBOR

N67-39510

(ACCESSION NUMBER)

34

(PAGES)

OR-89636

(NASA CR OR TMX OR AD NUMBER)

(THRU)

(CODE)

2.5

(CATEGORY)

THE UNIVERSITY OF MICHIGAN  
COLLEGE OF ENGINEERING  
Department of Aerospace Engineering

Progress Report

FLUID MECHANICS OF MAGNETICALLY BALANCED  
ARCES IN CROSS FLOWS

A. M. Kuethe

ORA Project 07912

supported by

NATIONAL AERONAUTICS AND SPACE ADMINISTRATION  
GRANT No. NGR-23-005-128  
WASHINGTON, D.C.

administered through

OFFICE OF RESEARCH ADMINISTRATION      ANN ARBOR

September 1967

## FOREWORD

The work described was carried out in the Gas Dynamics Laboratories of the Department of Aerospace Engineering. The personnel were: Professor Arnold M. Kuethe, Chief Investigator; Professors Richard L. Phillips and Stuart W. Bowen; Robert L. Harvey and Leland M. Nicolai, doctoral students; Ronald Kapnick and Richard Wallace, research assistants.

## TABLE OF CONTENTS

	Page
Summary of Activities (February 28, 1967 - August 28, 1967)	1
Program for Period (August 28, 1967 - March 1, 1968)	6
Personnel	7
Appendix A     The Fluid Mechanics of Magnetically Balanced Arcs in Cross-Flows	8
Appendix B     Spectroscopic Investigations of the Supersonic Air Arc	16
Appendix C     Preliminary Design of Magnetic Field Coils	22

## LIST OF FIGURES

	Page
Fig. 1. Schematic of free jet setup.	3
Fig. A1. Relative orientation of the velocity, magnetic, and electric fields.	9
Fig. A2. Qualitative model of balanced arc.	12
Fig. B1. Supersonic air arc spectrum. Run No. 545 - Mach No. = 2.5	20
Fig. C1. Example of magnet coil giving $B_z$ uniform to 1% over 10 cm arc length and 10 cm clearance between pole faces (dimensions in cm).	26
Fig. C2. Magnetic field properties.	28

## SUMMARY OF ACTIVITIES

February 28, 1967 - August 28, 1967

1. Some of the results and analyses are described in Appendix A, which is an abridged version of a paper by Arnold M. Kuethe, Robert L. Harvey and Leland M. Nicolai, now in final stages of preparation. The manuscript will be submitted to the AIAA Journal and a copy will be sent to NASA by early November. The most important results from the analyses of the experimental data are:

(a) The definition of a characteristic velocity for the analysis of the internal circulation by the conservation equations for the flow of a conductive fluid; (b) there is a range of parameters for the supersonic balanced arc within which non-equilibrium, Hall current, and radiation effects may be neglected and within which the Lorentz convection parameter (the ratio of Lorentz force to the viscous force on a representative element of the arc) is the most important similarity parameter governing internal flow.

2. Preliminary spectroscopic studies of the supersonic balanced arc are described in Appendix B. It is found that under some circumstances (not yet identified) Na and Cu atom lines are present in the column. The technique used is known as a slitless spectrogram, a method commonly applied to obtain spectra of lightning strokes.

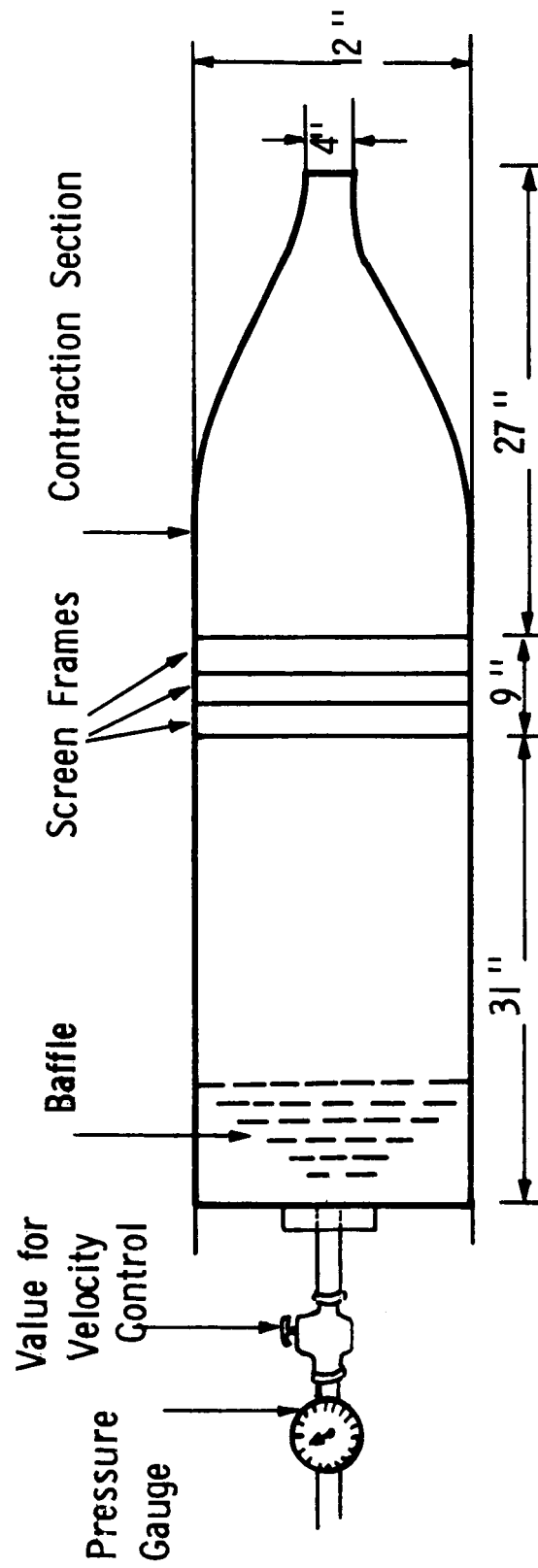
3. Preliminary design of magnetic field coils to provide a uniform field over the cross-section and length of balanced arcs in a subsonic free jet are described

in Appendix C. The setup is designed to check the influence of the boundaries of the cross-flow on the magnetic balancing and stabilization of arcs in cross-flow and to extend the investigations of Roman and Myers (Ref. 6 of Appendix A) toward a more detailed understanding of the mass, momentum, and energy transfer to the cross-flow. An improved electrode design, by Professor Richard L. Phillips will permit observation along the axis of the arc and will facilitate control of the flow along the arc axis; this latter feature is likely to be an important influence on the rate of mass transfer to the cross-flow.

4. The open jet wind tunnel for these studies has been designed and built by Richard Wallace under the supervision of Professor Phillips, and is now being calibrated. Using this tunnel, it will be possible to study the behavior of an electric arc in a stream of air and other gases, specifically argon, with velocities ranging from twenty to one hundred feet per second. Various adaptors will be fabricated to permit variation of the jet dimensions, thus permitting evaluation of the influence of the proximity of the jet boundaries on the dimensions, stability characteristics, and transfer properties of the arc.

The tunnel was designed to produce a low turbulence free jet with a nearly flat velocity profile. A schematic diagram with significant dimensions is shown in Fig. 1.

The tunnel's contraction section, settling chamber, screen frames, and the straight section, were fabricated from fiberglass. Fiberglass was used because it is easily fabricated into the required forms and is smoother and cheaper than other suitable materials.



Note : The entire tunnel has a square cross section

Fig. 1. Schematic of free jet setup.



The screens are bonded to their respective frames by epoxy. A special mounting technique was developed to insure that the screens would be flat and properly aligned. The screen frame was sandwiched between two larger pieces of plywood. First, the screen was carefully aligned with and fastened to the upper board which has a large (17 in. x 17 in.) square hole in it. This board is bolted to the other, with the screen frame in between. When the bolts are tightened, the screen draws tight across the frame. The epoxy is applied while the screen and screen frame are in their desired position. After the epoxy has cured, the excess screen, which is now fastened to the board and to the frame, is cut away. As a result the screen is secured in its desired position.

The working gas enters through a baffle which spreads the flow from its initial  $3/4$  square inch to a final 144 square inch cross section. The six plates of the baffle are perforated with  $1/2$  in. diameter holes. The holes are offset and hence cause the flow to expand. Plates range in size from 2 in. square to 12 in. square.

The stainless steel screens function in two distinctly different ways. First as in most wind tunnels, they remove turbulence by breaking the large eddies into smaller ones which decay more rapidly. All three screens perform this task. However, the first two screens are special. Since their pressure drop coefficient is very nearly equal to two, they will remove all velocity gradients and create an essentially flat velocity profile. Over one hundred and twenty-five pressure drop coefficients were calculated to find the most desirable screen.

Gaskets were formed from General Electric silicone rubber and used between all sections of the tunnel.

The tunnel is now completely assembled. The calibration data will yield turbulence levels and velocity gradients in the test section. Hopefully, the useful testing region will extend to about four inches away from the tunnel exit.

5. Robert L. Harvey and Leland M. Nicolai, doctoral students, have spent considerable time during the six months period on computer programs for various simplified models of the balanced arc. Preliminary results are being checked. The results will be incorporated in the authors' doctoral theses, copies of which will be sent to NASA.

**PROGRAM FOR PERIOD**  
**August 28, 1967 - March 1, 1968**

The detail design of the electrode assembly will be carried out and a set of coils to generate the external field will be built.

If sufficient funds and time are available the electrode assembly will be fabricated and the tunnel assembled for tests.

The first tests will involve balancing the arc in a closed tunnel and in an open jet of the same dimensions. The objective will be to determine the influence of the external stream boundaries on the arc properties. If the influence is appreciable, as it is likely to be if the arc blocks as much of the flow as it appears to in the Roman-Myers experiments, subsequent work will be directed toward determining the resulting effect of the boundaries on the transfer properties, including rate of loss of mass by the arc to the external flow.

Computer studies of the flow field in the case of the arc to determine the influence of the similarity parameters on the intensity of the internal circulation and on the temperature distributions will be continued.

Spot checks of some of the data at supersonic speeds will be made, directed particularly toward determining whether nonequilibrium effects can be identified with parameters such as pressure and arc current such that the Lorentz parameter is no longer the only similarity parameter for the arc properties.

## PERSONNEL

From January 1 to June 1, 1968, the period during which Professor Kuethe will be on sabbatical leave, the program will be under the supervision of Professors Richard R. Phillips and Stuart W. Bowen.

The thesis of Robert L. Harvey will probably be completed before January 1, 1968 and that of Captain Leland M. Nicolai will probably be completed during the summer of 1968.

## Appendix A<sup>†</sup>

### THE FLUID MECHANICS OF MAGNETICALLY BALANCED ARCS IN CROSS-FLOWS\*

Arnold M. Kuethe

#### INTRODUCTION

Our knowledge of even the gross aspects of mass, momentum, and energy transfer between an arc and an external stream depends today almost completely on empirical data. On the other hand, solutions to such practical problems as determination of the mass loss from a gaseous fission reactor, and the maximization of the acceleration in  $\vec{J} \times \vec{B}$  or  $\vec{E} \times \vec{B}$  accelerators will require detailed knowledge of fluid and plasma interactions such as occur at the boundary of a balanced arc. This paper identifies, through inference from the conservation equations and experimental data, some features of these mechanisms and the governing parameters.

The first instance of a steady arc balanced magnetically in a cross-flow of appreciable velocity was reported by Bond in 1962<sup>(2)</sup>. These experiments, in which fairly intense external magnetic fields were utilized to balance dc arcs in supersonic external flows were extended<sup>(3,4)</sup> and led to the determination of the gross properties of these arcs. One of these properties, a slant angle a few degrees greater than the Mach angle of the external flow was found to occur whenever the arc was steady; the cause of the slant is not known but Bond pointed out that the degree of ionization within the arc will be near its maximum if the arc slants at the Mach angle.

The experimental results described here utilized the same equipment as that for Refs. 2-4 and extends that work toward the delineation of a model of the arc as a basis for calculating its fluid mechanical structure. The configuration of the electric, magnetic, and flow fields is indicated in Fig. A1.

---

\*This account abstracts the work to be reported in Ref. 1. Preliminary results and studies were described in AIAA paper 67-96, by the same authors, presented at the 5th Aerospace Sciences Meeting, New York, January 23-26, 1967.

†This condensation was presented at the Midwest Conference on Mechanics, Fort Collins, Colorado, August 21-23, 1967 and will be printed in the Proceedings.

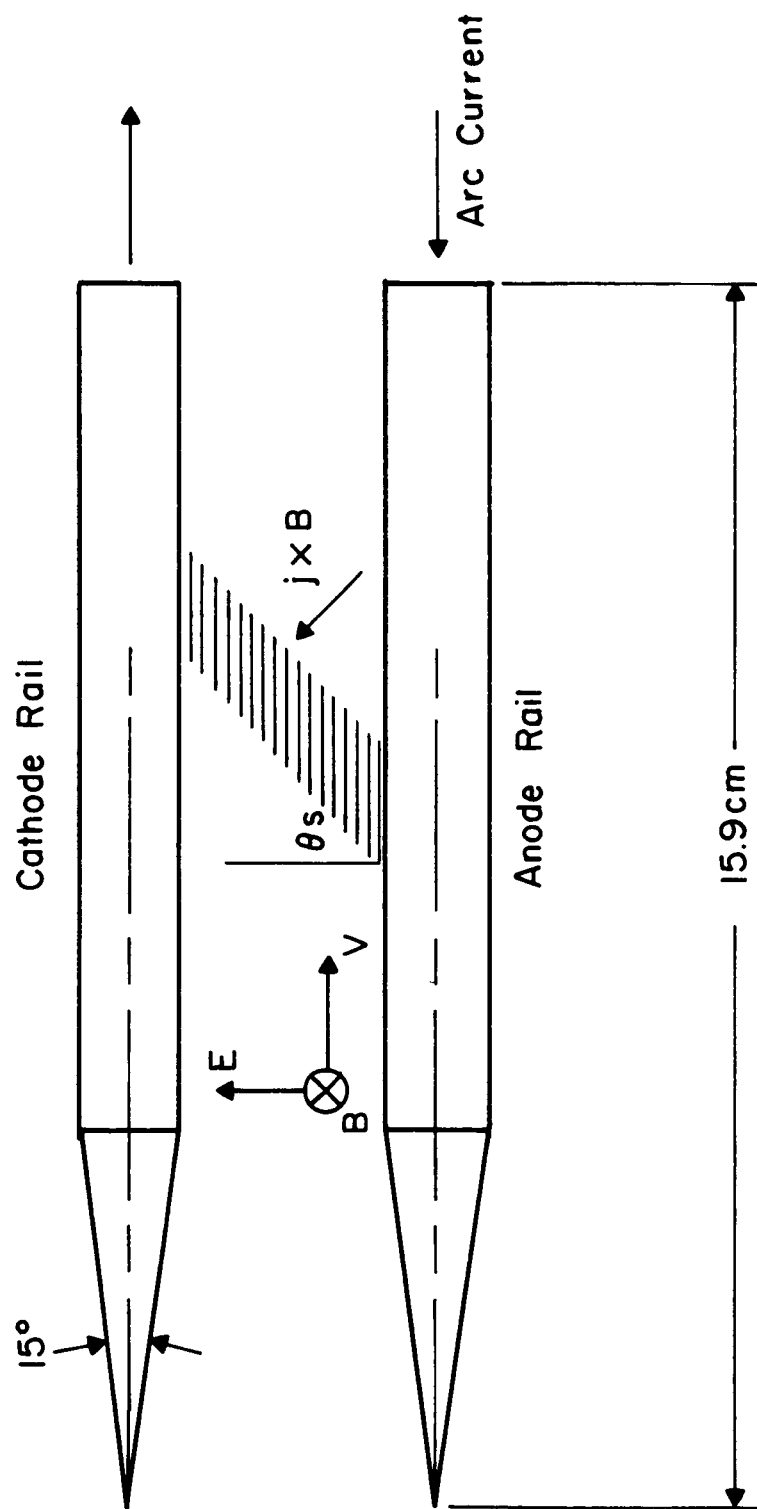


Fig. A1. Relative orientation of the velocity, magnetic, and electric fields.

The work of Roman and Myers<sup>(5, 6)</sup> shows that a steady arc normal to a subsonic cross-flow can be achieved when the arc is balanced magnetically in a free jet. The arc was remarkably steady, so that velocity distributions in the wake could be measured over a range of arc currents and jet speeds.

The first important conclusion relating to the fluid mechanical structure is that a steady arc has a central core which is impervious to the cross-flow; the bases for this conclusion are: (1) high speed motion pictures show that there exists an axial flow along the balanced arc in supersonic flow<sup>(1)</sup>, (2) a practically stagnant wake exists behind the arc in subsonic flow<sup>(5, 6)</sup>, (3) spectroscopic results indicate that the arc in a subsonic airflow was practically pure argon when that gas was injected at the cathode<sup>(5)</sup>.

The dimensions of the central impervious core were assumed to approximate those of the visible core of the arc, since the isotherm above which the radiation in the visible range is sufficient to expose the photographic film (5000 to 6000°K for air) is near the threshold below which the electrical conductivity and therefore the upstream Lorentz force on the fluid elements vanishes. The dimensions of the visible core of the arc were measured in both the subsonic<sup>(5, 6)</sup> and supersonic<sup>(1)</sup> experiments by a suitable arrangement of mirrors whereby two images approximately 90° apart were focused on the same frame of the film. These indicated that the arc cross-section was oval in the plane normal to the axis; the major axis was normal to the cross-flow direction and 1.3 to 1.8 times the minor (streamwise) axis.

Some limited attempts have been made<sup>(7, 8, 9)</sup> to attack the problem of the balanced arc by solving the conservation equations for the entire flow field with boundary conditions at infinity. The complete solution would comprise determination of the flow fields, internal and external, for a plasma column whose dimensions are determined by the conditions for equilibrium between the internal and external pressure fields. The solution is incomparably more difficult than that of determining the flow field around a bluff body of fixed dimensions. For the

arc, even if the cross-section shape were known, the boundary conditions necessary for calculating the flow in the boundary layer, and particularly near the flow separation point, are unknown. One is accordingly forced to seek a model of the arc which will provide a framework for calculating arc properties susceptible of experimental check.

The experiments at subsonic and supersonic speeds suggest the qualitative model shown in Fig. A2; the model incorporates the oval or elliptical cross-section broadside to the flow, flow separation at the maximum section and the near stagnation wake, and an internal circulation set up by differential Lorentz forces generated by a constant magnetic field and a nonuniform current density over the cross-section. The indicated mass transfer from the arc to the external stream would occur when the fluid elements near the boundary are cooled sufficiently so that the current density and therefore the Lorentz force decreases sufficiently so that the element is swept downstream.

### SIMILARITY PARAMETERS

We assume that because of the internal circulation the properties over the central core are sufficiently uniform so that density variations can be neglected and the viscosity coefficient  $\mu$ , the heat conductivity  $k$ , the specific heat at constant pressure  $c_p$  are assumed constant. The nondimensional momentum, energy and continuity equations become

$$\frac{d\vec{u}}{dt} = -\nabla p + j\vec{e}_x + \frac{1}{\sqrt{L_c}} \nabla^2 \vec{u} \quad (1)$$

$$\frac{d\theta}{d\tau} = \frac{1}{Pr_1 \sqrt{L_c}} \nabla^2 \theta + \frac{EI/k_1 T_1}{Pr_1 \sqrt{L_c}} j \quad (2)$$

$$\text{div } \vec{u} = \frac{\epsilon d}{U_1 \rho_1} \quad (3)$$

where  $\vec{u} = \vec{V}/U_1$  ( $U_1$  is a characteristic velocity),  $p = P/\rho U_1^2$  ( $P$  is the pressure),  $j = J/J_1$  ( $J_1$  is a characteristic current density),  $\theta = T/T_1$  ( $T_1$  is a characteristic



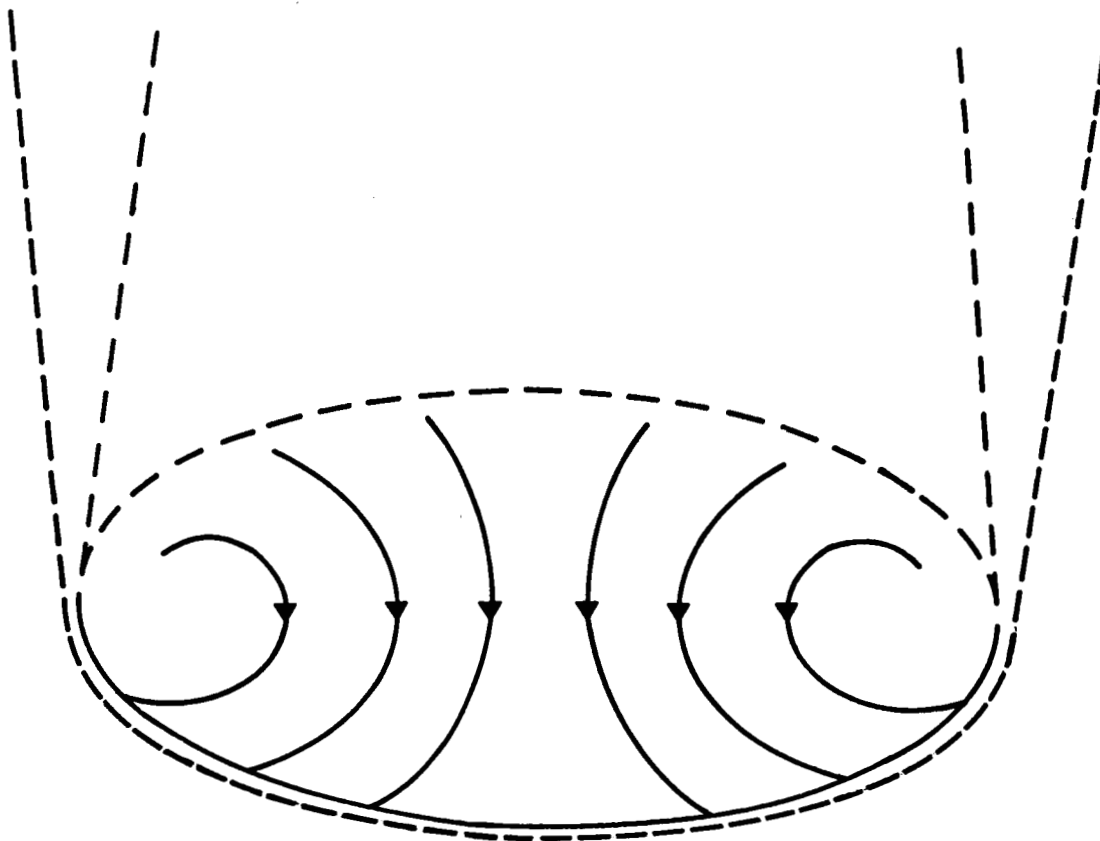
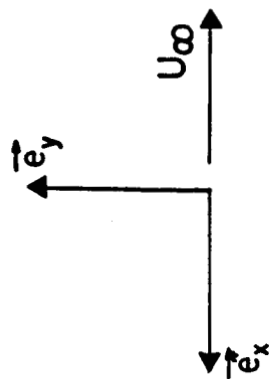


Fig. A2. Qualitative model of balanced arc.

temperature),  $L_c = \rho_1 I B d_s / \mu_1^2$  ( $I$  is the arc current,  $B$  the magnetic field intensity,  $d_s$  the minor axis of the arc cross-section),  $Pr = c_{p1} \mu_1 / k_1$ ,  $E$  is the voltage drop along the arc,  $\bar{e}_x$  is the unit vector in the  $x$  direction, and  $\epsilon$  is the "sink strength" representing the difference between the rate at which mass is supplied by the axial flow and the rate at which mass is transferred to the boundary. The internal velocities are assumed small compared with sonic speed and the viscous dissipation is neglected. Also, effects of radiation, of departures from equilibrium in the arc plasma and of Hall currents are neglected.

The values of  $J_1$  and  $T_1$  are average values over the visible cross-section and  $c_{p1}$ ,  $\rho_1$ , and  $k_1$  are corresponding properties.

The "Lorentz convection parameter"  $L_c$  is the ratio of the Lorentz force on a representative fluid element to the viscous force; it is therefore analogous to the Grashof number in free convection. Further, except for effects of joule heating, the circulation within the arc core is closely analogous with that resulting from gravity forces within a centrally heated horizontal cylinder of gas.

A suitable characteristic velocity, as indicated by the experimental results, is

$$U_1 = \sqrt{J_1 B d / \delta_1}$$

The ratio  $U_1 / U_{\infty}$  ( $U_{\infty}$  is the velocity component of the external flow normal to the arc) is found to be constant for the subsonic tests of Roman and Myers, and another constant for the supersonic tests at Mach numbers 2.5 and 3.0.

The experimental results at Mach numbers 2.5 and 3.0 show that  $E I / k_1 T_1$  (the ratio of the rate of joule heating of a representative element,  $EJ$ , to the rate at which heat is conducted from the element  $k_1 T_1 / d^2$ ) is proportional to  $\sqrt{L_c}$  over a wide range of operating conditions. On the basis of Eqs. (1) and (2) it is therefore concluded that there exists a range of conditions for which the Lorentz convection parameter is the governing parameter for the internal flow.

The above proportionality breaks down for the Mach 3.5 and for the subsonic experimental results of Roman and Myers. For the former, this anomalous

behavior is consistent with appreciable nonequilibrium effects in the form of a high electron temperature compared with the gas temperature; the low ambient pressures of 0.01 to 0.02 atmospheres favor this explanation. For the subsonic experiments of Roman and Myers the small dimensions of the free jet (2 x 2 in.) and the resulting high effective "blockage ratios" for the arc (up to 0.5) indicate that the anomalous behavior may result from the effects of large and variable jet boundary interference on the dimensions and properties of the arc.

## CONCLUSIONS

The conclusion is drawn that there exists a range of operating conditions for which the steady magnetically balanced arc in a cross-flow may be treated as a central impervious core of relatively uniform properties. Within this range the conservation equations for flow of a conducting fluid under equilibrium conditions with negligible Hall effects are valid to a good approximation in the core; the transfer of mass, momentum, and energy to the external flow then takes place through a relatively thin boundary layer.

## REFERENCES

1. Kuethe, A.M., Harvey, R.L., and Nicolai, L.M., "The Fluid Mechanics of Magnetically Balanced Arcs in Cross-Flows," to be published in AIAA Journal. Preliminary results were presented in AIAA paper 67-96 by the same authors.
2. Bond, C.E., "Magnetic Confinement of an Electric Arc in Transverse Supersonic Flow," AIAA J., 3, 142 (1963).
3. Bond, C.E., "The Magnetic Stabilization of an Electric Arc in Supersonic Flow," Ph.D. dissertation, The University of Michigan (1964), also ARL-65-195, October, 1965.
4. Bond, C.E., "Slanting of a Magnetically Stabilized Electric Arc in Transverse Supersonic Flow," Phys. Fluids, 9, 705 (1965).
5. Roman, W.C., "Investigation of Electric Arc Interaction with Aerodynamic and Magnetic Fields," Ph.D. dissertation, Ohio State University (1965).
6. Roman, W.C. and Myers, T.W., "Investigation of Electric Arc Interaction with Aerodynamic and Magnetic Fields," ARL 66-0191, Aerospace Research Laboratories, 1966. See also AIAA Paper 67-98 (1967).

7. Broadbent, E.G., "Electric Arcs in Cross Flow," Royal Aircraft Establishment Technical Memo No. 897, 1965.
8. Fischer, E. and Uhlenbusch, J., "Interactions of Free Burning Arcs with Transverse Gas Flows in Magnetic Fields," Report HMP 110, Technical University, Aachen, West Germany, January 1967.
9. Myers, T.W. and Roman, W.C., "Survey of Investigations of Electric Arc Interactions with Magnetic and Aerodynamic Fields," USAF Aeronautical Research Laboratories, ARL 66-0184, September, 1966.

## Appendix B

### SPECTROSCOPIC INVESTIGATIONS OF THE SUPERSONIC AIR ARC

Stuart W. Bowen

#### INTRODUCTION

Several questions of particular interest in understanding the various physical mechanisms important to the transversely blown arc in air are:

1. What is the origin of the radiation emanating from the arc.
2. Can this radiation be used to infer properties of interest such as temperature, species density, degree of ionization and the variation of these properties along the arc.
3. Are these measurements consistent with arc properties previously inferred from current and voltage measurements and in particular does the assumption of LTE appear reasonable.

A simple spectroscopic investigation in the visible spectral range of the supersonic air arc has been initiated with the objective of answering these questions.

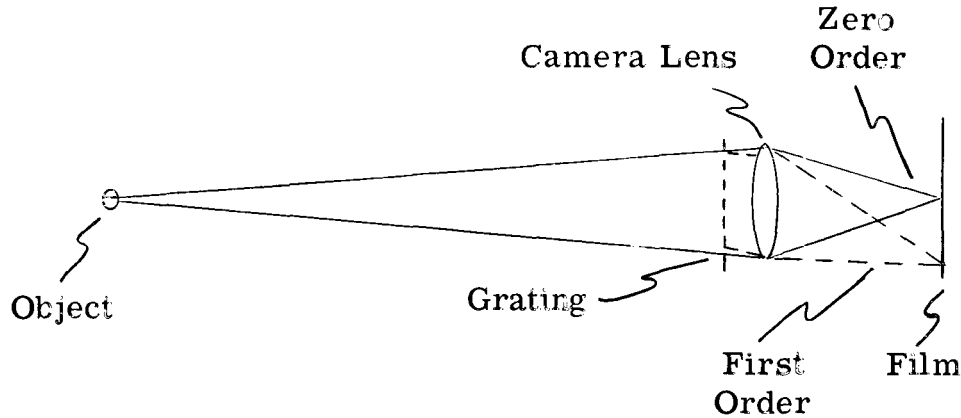
Only the first question has so far been answered. Some progress has been made on the second while the third question of course hinges on the outcome of the second.

#### EXPERIMENTAL PROGRAM

After initiation by the firing wire the arc moves to an equilibrium position in the tunnel where the drag and Lorentz forces are balanced. Because of unavoidable variations in the experimental conditions from run to run, the equilibrium position of the arc cannot be precisely predicted. Conventional spectroscopic techniques wherein the arc image is focussed onto the spectrograph slit were tried, but the uncertainty in predicting the arc position was large enough so that the arc image did not fall on the slit.

The arc is a long thin phenomena so that the technique known as a slitless spectrogram used to obtain lightning stroke spectra suggested itself.

In this method a conventional camera is preceded by a dispersing element such as a transmission grating.



By suitably orienting the grating rulings parallel to the lengthwise dimension of the arc image, one obtains a series of monochromatic images of the arc which include the zero order with the first order spectra, arrayed on both sides of the zero order image. The camera lens then focusses these images onto the film. Usually only the zero order and first order spectra on one side can be included in field of the camera lens. One moves as far away from the object as possible so as to provide a smaller arc image and hence higher spectral resolution as well as to make the extreme rays passing through the edges of the grating more nearly parallel.

If  $\Delta\lambda$  is the spectral resolution and  $\Delta x$  is the arc image width on the film then  $\Delta\lambda = (d\lambda/dx) \Delta x$  where  $d\lambda/dx$  is the reciprocal dispersion provided by the grating-lens combination. For the present case a 50 mm f/1.5 lens was used in conjunction with a 590 line/mm grating giving  $d\lambda/dx = 337 \text{ \AA}/\text{mm}$  in the first order. The resulting spectral resolution is about  $30 \text{ \AA}$  for a 1 cm diameter arc at  $10^3$  focal lengths or 50 meters, i. e.  $\Delta x = .1 \text{ mm}$  on film. A Nikon 35 mm camera having a motor drive is used to give 4 frames/sec. Typical exposures are 1/250 sec at f/1.5.

The blackening along the spectral "line" represents the spectral intensity along the arc length.

Note that the lack of a slit obviates the necessity of accurate positional prediction.

Wavelength calibration is provided by photographing rare gas discharge tubes (Plucker Tubes) and plotting wavelength vs. distance on the film measured from the zero order image. A measuring engine having an accuracy of  $\pm 1\mu$  is used for the measuring. The precision achieved is much less, being limited by the arc image size on the film. The Plucker tube is placed at the same distance from the lens as the arc.

Intensity calibration is obtained by photographing the flat tungsten filament of a standard pyrometric lamp placed at the arc distance. Correction must be made because the angular width of the tungsten filament may differ from the arc. Based on previous similar calibrations, film density or blackening as a function of intensity and wavelength can be expected to yield an absolute intensity calibration accurate to  $\pm 20\%$ . A recording microdensitometer is available.

## PRELIMINARY RESULTS

The arc radiation is from both the electrode spots and the arc column. The spot radiation consists of a metallic spectrum characteristic of the firing wire and electrode material.

The column radiation is mainly molecular band radiation from the first negative system of the  $N_2^+$  molecule. The transition is  $2\sum_u^+ \rightarrow 2\sum_g^+$ . The vibrational bands seen are  $v', v'' = 0, 0; 1, 1$ , the  $\Delta v = v'' - v' = +1$  sequence (0, 1; 1, 2; 2, 3 etc), and a somewhat fainter  $\Delta v = +2$  sequence ( $v', v'' = 0, 2; 1, 3$  etc). The individual rotational structure is not resolved within the bands.

No other band systems which might be present in hot air are seen in the range 3800-6500 Å. The lack of  $O_2$  Schuman-Runge, NO Beta bands or a strong continuum (0- free-bound) seem qualitatively consistent with the radiation expected from air in the range 7000-10,000 °K and  $\rho/\rho_0 \sim 10^{-3}$  (Ref. 1).

Some Na and Cu atom lines are also present in the column. Sodium is a very common impurity, while the copper comes from both the firing wire and the electrodes. The presence of these lines in the column indicates that under some conditions electrode material is introduced into the column. The metallic lines are not always present in the column however, but when they are present they will provide another convenient measure of temperature.

One further question arising because of the metallic atom in the column is whether the assumption of pure air, used in relating the measured conductivity to a temperature, is reasonable. The impurities seen are more easily ionized than air and at low temperatures will supply most of the free electrons. At higher temperatures most of the electrons come from the air itself and the presence of small amounts of metallic impurities does not affect the pure air assumption. The quantity and kind of impurity are both important as well as the temperature and further study is contemplated.

An example of the slitless spectra is included as Fig. B1. Because the grating rulings were not parallel to the arc, the dispersion was not perpendicular to the spectral lines and therefore this particular spectrogram is suitable only for qualitative purposes.

One further feature should be noted. Successive spectra taken at 1/4 sec intervals of the arc do not exhibit large differences in either the intensity or nature of the radiation from the column. The assumption of steady state conditions during a run may therefore be quite reasonable.

## FUTURE WORK

The  $N_2^+$  first negative system so far appears usable for possible measurements of (a) the absolute intensity yielding an electronic excitation temperature and (b) the vibrational energy distribution of the  $\Delta v = 0$  and  $\Delta v = 1$  sequences, yielding vibrational temperature of  $N_2^+$ . The rotational energy distribution is probably no longer a strong enough function of temperature to be usable over the limited range of any one band which is free from the interference of other bands.





5218 } Cu I  
553  
5105

N<sub>2</sub>O, 2, 4709 Å

N<sub>2</sub><sup>+</sup> O, 1, 4278 Å

N<sub>2</sub><sup>+</sup> O, 0, 3914 Å

It is hoped to calculate the radiant emission from the  $N_2^+$  first negative system and then plot a series of curves showing the spectral emission as a function of wavelength for temperatures of interest with the spectral resolution expected. Comparison with the measured intensity distribution will then be quite simple.

The copper lines which are present in the arc will provide further indications of LTE.

Reference 1. "Radiant Emission from High Temperature Equilibrium Air," Breene, R.G. and Nardone, M., J. Quant. Spect. Rad. Transfer, Vol. 2, 1962, p. 273.

or

General Electric Space Sciences Lab Tech. Infor. Series R615D020, May 1961.

## Appendix C

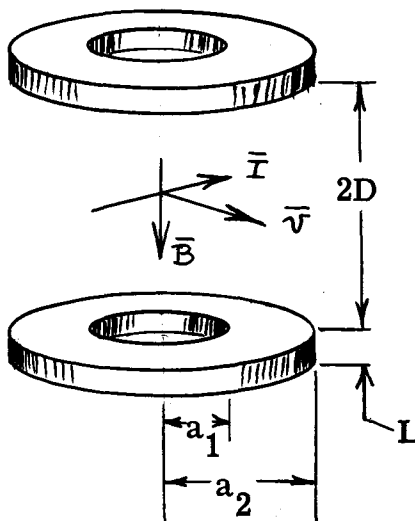
### PRELIMINARY DESIGN OF MAGNETIC FIELD COILS

Stuart W. Bowen

#### Introduction

The detailed study of the structure, transfer mechanisms and stabilization of an arc in a cross flow requires close control of the perpendicular flow, current and magnetic field vectors. The generation of a uniform external magnetic field, over the region of the arc in the cross flow, by means of magnetic field coils is considered here. A maximum deviation from uniformity of  $.01 B_z$  over this region was considered consistent with the other features of the tunnel design. The magnetic field is oriented so that  $\bar{I} \times \bar{B}$  is opposite to  $\bar{v}$  and the design value of  $B_z = C_D \rho v^2 D_{\text{arc}} / 2I$ . If we assume  $C_D \approx 1.0$ ,  $B_z = 100$  gauss will balance a 500 amp arc having a diameter of 1 cm against a speed of about 30 m/sec at atmospheric pressure.

One simple method for providing this field is by the use of a pair of air core field coils with their axis perpendicular to the plane of  $\bar{v}$  and  $\bar{I}$ .

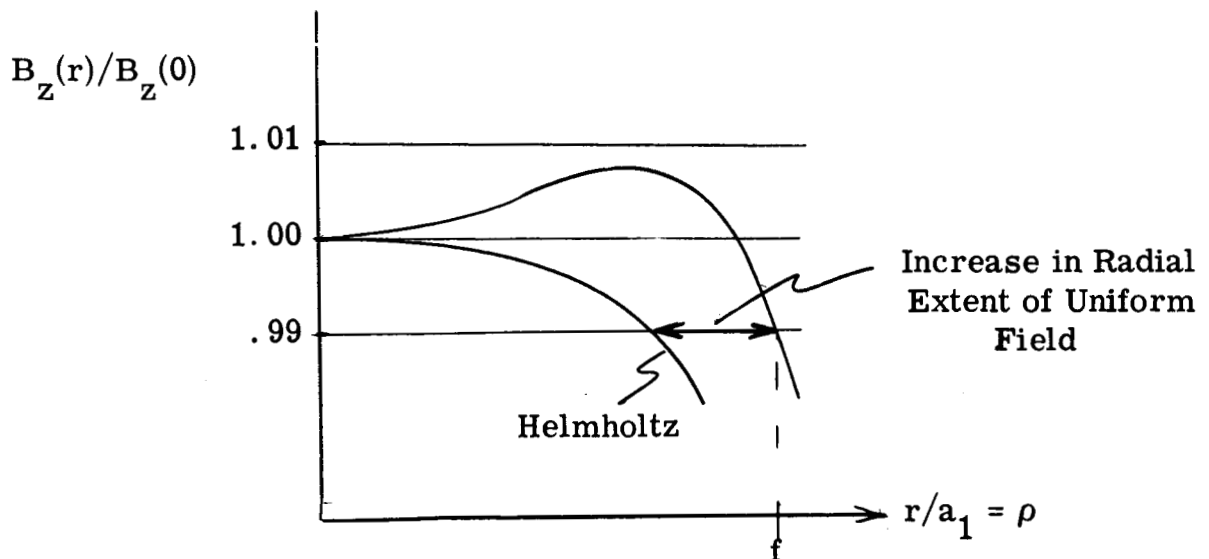


The central holes in the coils can be used to view the arc perpendicular to the flow.

For simplicity only uniform current density rectangular cross section co-axial circular coils were evaluated. The plane defined by the arc current and flow velocity vectors was taken to be midway between the coil faces.

A Helmholtz pair immediately suggests itself as a coil configuration giving a very uniform axial field component. The Helmholtz configuration positions the two coils so that  $\partial^2 B_z / \partial z^2 = 0$  midway between the coil pair, but unfortunately provides a uniform axial field only over a rather limited central region. The off axis value of  $B_z$  decreases from the value on axis, falling below  $.99 B_z$  ( $r = 0$ ) at a very small fraction  $f$  of the inner coil radius  $a_1$ . The requirement for sufficiently uniform  $B_z$  over a given arc length  $\ell = 2fa_1$  would therefore require extremely heavy, large diameter cumbersome and expensive coils.

By relaxing the Helmholtz spacing restriction, one finds that the off axis mid plane  $B_z(r)$  can be made first to increase slightly and then decrease, yielding a fractional radius  $f = r/a_1$ , at which the field has deviated by 1% from the central value, that is substantially increased over the Helmholtz configuration.



Since this fractional radius corresponds to a given physical arc half length, the scale of the coils can be correspondingly reduced.

The precise nature of the shape of the  $B_z(r)/B_z(0)$  curve as a function of  $\rho = r/a_1$  depends on the nondimensional coil thickness  $\lambda = 2L/a_1$  ( $L$  is the physical coil thickness), the outer to inner coil radius ratio  $\alpha = a_2/a_1$ , and the nondimensional coil spacing  $\delta = D/2a_1$  where  $D$  is half the distance between inner coil faces. Thus  $f = f(\alpha, \lambda, \delta)$ . Variation of the parameters  $\alpha$ ,  $\lambda$  and  $\delta$  allow one to vary the fractional radius and maximize it. However using this fraction radius together with  $\alpha$ ,  $\lambda$  and  $\delta$  one can then express other parameters of interest such as coil mass, power required for a given magnetic field, current, voltage coil heating rate (power/mass) as functions of  $\alpha$ ,  $\lambda$ ,  $\delta$ , the coil material properties such as density, conductivity, etc., and the dimensional distance  $\ell = 2fa_1$  over which the given field uniformity is required. Rather than simply maximizing  $f$  as a function of  $\alpha$ ,  $\lambda$  and  $\delta$ , one can now optimize the effects of each of these quantities of interest or, for instance, minimize the coil weight while keeping the power, heating rate current and voltage within usable bounds for a given clearance between the coil faces.

Because the axial magnetic field at an off axis point must be found by numerical quadrature the entire optimization procedure must be performed numerically.

### Magnetic Field Calculations

The calculation of  $B_z(r, z)$  resulting from a thick finite coil has been programmed for digital computation using the formulas given in Ref. 1. The field can be calculated at any point within the volume bounded by the inner coil radius and the coil faces by summing the contribution due to each coil. A program was also prepared which links the IBM 7094 to a Calcomp digital plotter, yielding inked graphs of the magnetic field. Other quantities such as the angle between the total field vector and the  $z$  axis, the nondimensional values of mass, power, voltage, current and rate of temperature rise are printed out as functions of the coil configuration parameters.

In the process of writing the above very extensive program the field and field angle produced singly and in pairs by the following coil configurations were also programmed:

1. Loop with negligible cross section.
2. Finite sheet solenoid.
3. Washer having negligible thickness.

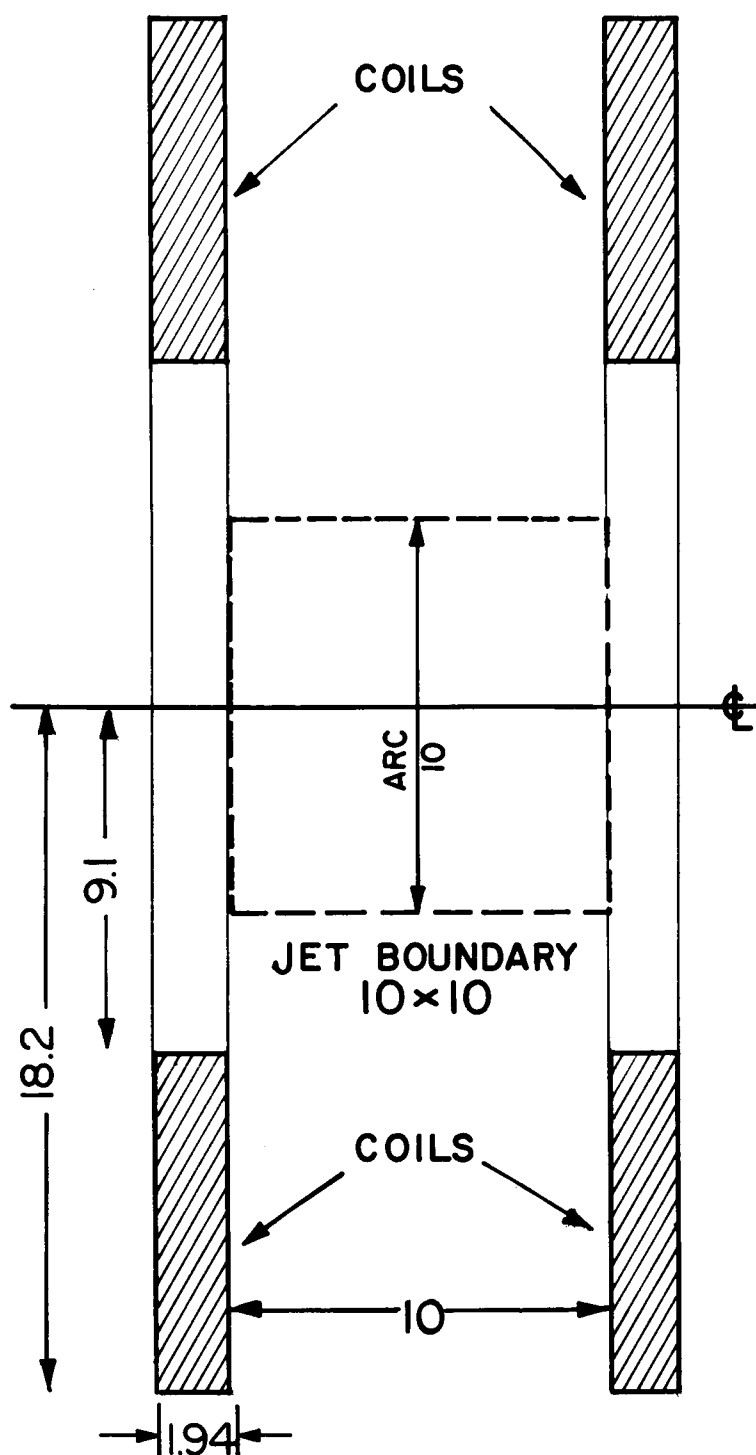
In these calculations the finite coil construction was taken to be a thin copper strip wrapped together with an insulating mylar tape in a radial spiral.

### Preliminary Results

The calculations are not yet complete but a few preliminary conclusions have appeared.

1. It is possible to produce  $B_z$  uniform to 1% over as much as 50% to 60% of the inner coil radius, consistent with the required coil separation, which here requires  $\delta \geq f$ .
2. The optimal coil shape for minimum mass consistent with reasonable values of current, power, etc., appears to be a very thin pancake coil almost like a washer with an outer to inner radius ratio on the order of 2 and a thickness to twice inner radius ratio on the order of .10. The optimal spacing between the coil faces divided by the inner coil radius is then about 1.
3. The values of current, voltage, power, and temperature rise for the magnetic fields required ( $B_z \approx 100$  gauss over an arc length of 10 cm) are quite reasonable.
4. The  $B_z$  curves as functions of  $\rho = r/a_1$  in planes away from the mid plane slowly develop an off axis ear as one moves toward one coil face but reasonably uniform values of  $B_z$  (i. e. less than a few percent variation) are found for planes as much as half way to one coil face.

As an example, the configuration shown in Fig. C1 will produce 100 gauss uniform to 1% over a 10 cm length ( $\pm 5$  cm radius) in the mid plane of the coils and give  $\sim 10$  cm clearance between the coil faces. The coil construction was taken to be a 5 mil copper strip wrapped together with a 3 mil mylar insulating tape. While this design is probably not the best that can be done, it would



$B$  at Center = 100 GAUSS  
 Current  $I$  = 3.42 AMP  
 Voltage  $V$  = 14.3 Volts  
 Power  $P$  = 49 Watt/Coil  
 Mass  $M$  = 9.1 Kg/Coil  
 $dT/dt$  Rate of = 0.05 °C/sec  
 Temp Rise

$\alpha$  = 2.0  
 $\lambda$  = .1075  
 $\delta$  = .55  
 $f$  = .55

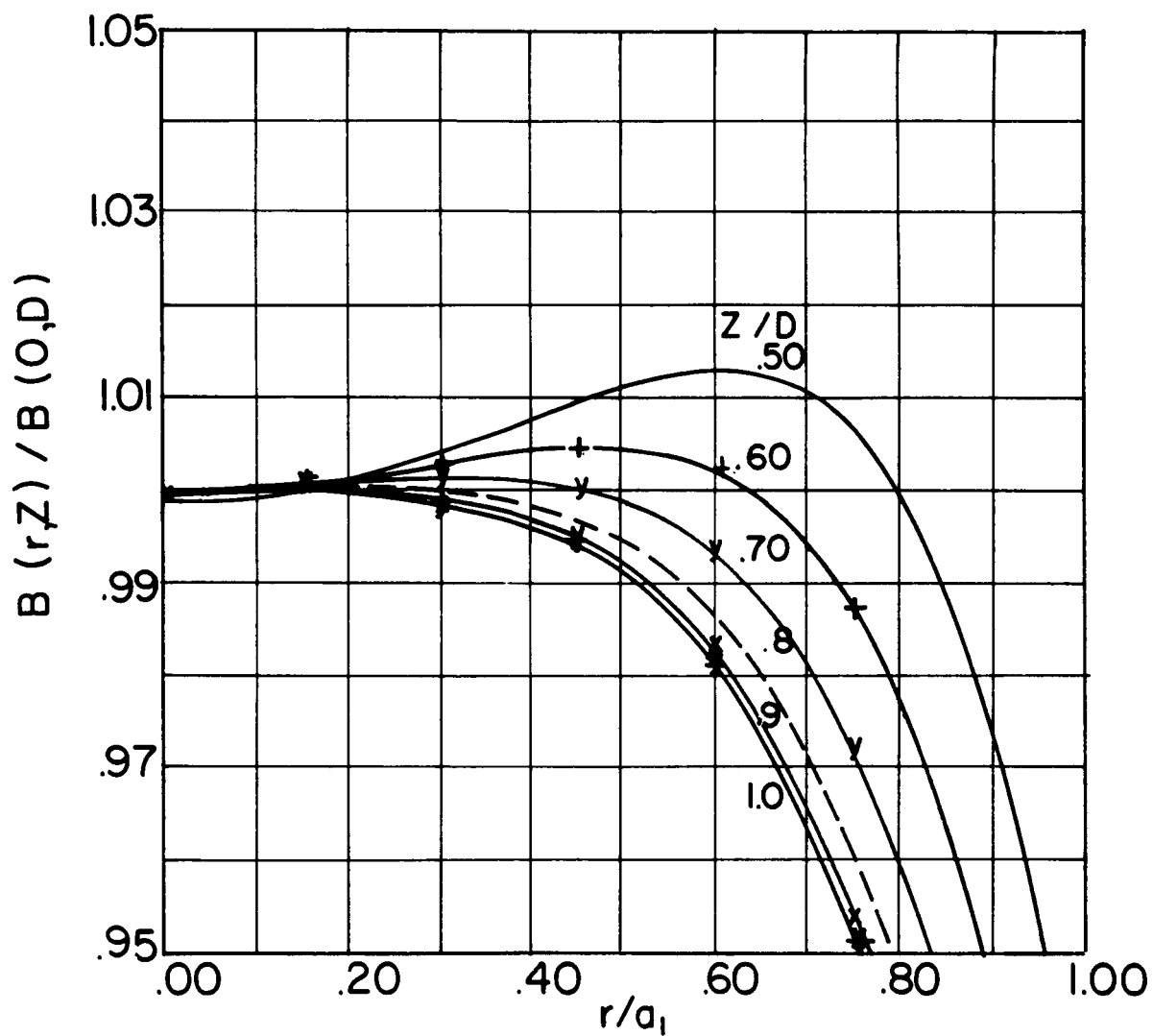
Fig. C1. Example of magnet coil giving  $B_z$  uniform to 1% over 10 cm arc length and 10 cm clearance between pole faces (dimensions in cm).

provide a feasible coil pair. As a matter of interest the coil weight required to produce a uniform field over a given arc length was decreased by a factor of 30 over the configuration initially tried.

As an example of the magnetic field calculations, the value of  $B_z(r, z)$  (nondimensionalized by  $B_{oo}/j\mu a_1$ ,  $j$  = current density in coil,  $a_1$  = inner coil radius,  $B_{oo}$  is field at center,  $\mu$  = permeability) as a function of  $r$  (nondimensionalized by  $a_1$ ) for various different planes is shown in Fig. C2. The value  $z_1/D = 1.0$  refers to the mid plane, halfway between the two coils, and  $z_1/D = .50$  is the plane halfway from the center to one coil face. Although  $\lambda = .5L/a_1 = .125$  here, the field for  $\lambda = .1075$  is nearly the same.

Reference 1. Axial and Radial Magnetic Fields of Thick Finite Length Solenoids, G. V. Brown, L. Flax, E. C. Hean, J. C. Laurence, NASA TR R-170, December 1963.





$a/a_1 = 2.0$   
 $B(0,D) = 0.1259$

$D/a_1 = 0.55$   
 $L/a_1 = 0.0625$

Fig. C2. Magnetic field properties.